

Temporal and spatial variations in hydro-geochemistry of cave percolation water and their implications for four caves in Guizhou, China

LUO Weijun^{1,2}, WANG Shijie^{1,2*}, XIE Xingneng¹, ZHOU Yunchao¹, and LI Tingyu^{1,2}

¹ State Key Laboratory of Environmental Geochemistry, Institute of Geochemistry, Chinese Academy of Sciences, Guiyang 550002, China

² Puding Karst Ecosystem Research Station, Chinese Academy of Sciences, Puding 562100, China

* Corresponding author, E-mail: wangshijie@vip.skleg.cn

Received March 3, 2012; accepted April 3, 2012

© Science Press and Institute of Geochemistry, CAS and Springer-Verlag Berlin Heidelberg 2013

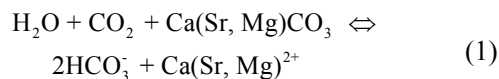
Abstract Soil water and cave drip water from four cave systems in Guizhou, Southwest China, were monitored and sampled monthly from April 2003 to May 2004 to understand spatio-temporal variations in hydro-geochemistry of cave percolation water. The results indicated that among the 5 drip water sites from the Liangfeng Cave (LFC), there were no significant differences among the hydro-geochemical parameters. In the Xiniu Cave (XNC), the drip rates were variable and responded quickly to precipitation events in the 3# (No. 3) drip site with variable water head; both bulk and variation in drip rates were smaller in the 2# with constant water head. However, in the Qixing Cave (QXC) and Jiangjun Cave (JJC), drip rates, concentrations of major ions and saturation index for calcite (SI_c) were smaller, and Mg/Ca ratios in Group I (1#, 2#, 6#, 7# and 8# in the QXC; 2# and 3# in the JJC) were larger than those in Group II (3#, 4#, 5# and 9# in the QXC; 1# and 4# in the JJC). These differences might be the result of different hydrogeological processes above the caves, which are divided into five categories based on hydro-geochemistry data. The formation of some proxies in speleothem, such as Mg/Ca, is likely to be affected by those processes.

Key words cave drip water; hydro-geochemistry; paleo-climate; karst; Guizhou, China

1 Introduction

Calcite in speleothem is one of the most important geological archives for studying paleo-climatic changes with the development of high-resolution dating of stalagmite (TIMS on the basis of U-Th disequilibrium (Wang Zhaorong et al., 1999, 2001). However, there are different interpretations when recovering and reconstructing paleoclimate using speleothem, because the formation of speleothem is affected to varying degrees by a number of hydro-geochemical factors. For example, there are significantly different stable isotope ($\delta^{13}\text{C}$, $\delta^{18}\text{O}$, etc.) values for coeval speleothem from different sites of the same cave (Linge et al., 2001; Serefiddin et al., 2004), which reduces the comparability among different research results. The primary geochemical process, i.e., the forming process of major environmental proxy indicators such as Mg/Ca ratio, carbon isotopes and oxygen isotopes in

karst cave systems, can be summarized as follows (Dreybrodt, 1988; Ford and Williams, 2007):



In addition to climatic factors such as temperature and precipitation, the lithological characteristics of the strata overlying the cave can also affect this process. Cave percolation water is a carrier of the information about the formation and evolution of environmental proxy indicators in speleothem. In addition to climatic factors, their hydro-geochemistry is controlled by residence time and water flow path in the overlying cave. Consequentially, different paths, such as pipe flow, diffusion flow, and matrix flow, would lead to different hydrodynamic mixing mechanisms

(Tooth and Fairchild, 2003). Therefore, the flow rate, the concentrations of various elements, and the isotope signals of percolation water can be affected (Baker and Bradley, 2010; Fairchild and Treble, 2009; Fairchild et al., 2006; McDonald and Drysdale, 2007; McDonald et al., 2007; Tooth and Fairchild, 2003). In this sense, each cave has its unique features (Spötl et al., 2005). Therefore, for paleo-climatic reconstruction, it is important to study the inherent variations in hydro-geochemistry of cave drip water (Baldini et al., 2006; Bradley et al., 2010; Lambert and Aharon, 2010, 2011).

Here are reported the observations from four cave systems in Guizhou Province, Southwest China. Significant statistical differences were noticed in the hydro-geochemical indices from different drip sites of QXC (He Yaoqi et al., 2005; Zhou Yunchao et al., 2005) and JJC, whereas those indices were not so different in LFC which is located around the Dongge Cave (Yuan et al., 2004) and XNC. Therefore, those four cave systems have proved themselves to be ideal for studying temporal and spatial variations in hydro-geochemistry of cave percolation water.

2 Study sites

Guizhou Province is located in the center of a continuously distributed karst region in East Asia, which is one of the three largest karst regions in the world. Due to certain geological and geomorphological conditions and a humid climate, in this region there have developed cave systems and valuable speleothem for us to restore and reconstruct pa-

leo-environments during the Quaternary in South China. Much work has been done on paleo-climate reconstruction using speleothem in this area (Dykoski et al., 2005; He Yaoqi et al., 2005; Kelly et al., 2006; Wang et al., 2005; Yuan et al., 2004; Zhou Yunchao et al., 2005).

The four caves are located in the watersheds of the Yangtze River and the Pearl River (Fig. 1), and they are very different in bedrock geology, vegetation coverage, and climatic characteristics (Table 1).

3 Methods

Approximately 100 kg NaCl was buried near the soil water sampling sites, and ten sites were chosen to bury NaCl in the soil overlying each cave in June 2003 to trace the residence time of cave percolation water in the overlying cave.

Samples used in this study include soil water, spring water and drip water. Cave drip waters were collected from drip sites in the main channels of the caves (Fig. 1). Soil water was collected at the depths of 50 and 100 cm from the soil overlying the caves (detailed sampling methods can be seen in Fig. 2). The spring water samples were collected nearby each cave (Fig. 1). All water samples were collected monthly by means of a 0.45 μm membrane filter (Millipore). A small portion of each sample was stored to measure anions, and the remainder was acidified with ultra-purified nitric acid to pH<2 to measure cations. The samples were refrigerated (4°C) prior to measurement.

Table 1 General information about the four caves

	LFC	QXC	JJC	XNC
Site	Libo	Duyun	Anshun	Zhenning
Longitude	108°03'E	107°16'E	106°04'E	105°47'E
Latitude	25°16'N	25°59'N	26°17'N	26°04'N
Altitude of cave entrance (m)	580	1 020	1 360	1 300
Lithology	Limestone	Dolomitic-limestone	Dolomite	Dolomite
Stratum age	Middle and Upper Carboniferous	Lower and Middle Carboniferous	Lower Triassic	Lower Triassic
Vegetation	Karst primary forest	Brushwood	Scrub tussock	Thorn tussock
Soil thickness (cm)	27 (0–135)	33 (6–180)	26 (0–130)	21 (0–55)
Soil tightness	Loose	Tight	Very loose	Very tight
Soil texture	Loamy	Clay	Loamy	Clay
Soil hole	Moderate	Small	Moderate	Small
Roof thickness overlying the cave (m)	80–140	50–90	50–60	20–60
Bedrock fracture	Large	Small	Large	Small
Mean annual temperature (MAT) (°C)	18.6	16.6	14.0	15.4
Annual precipitation (mm)	1 118.7	1 185.1	936.9	932.6
Mean cave air temperature (°C)	15.1±1.3	13.5±1.7	14.5±1.1	17.0±1.2
Mean cave air relative humidity (%)	98±2	98±2	98±2	99±1

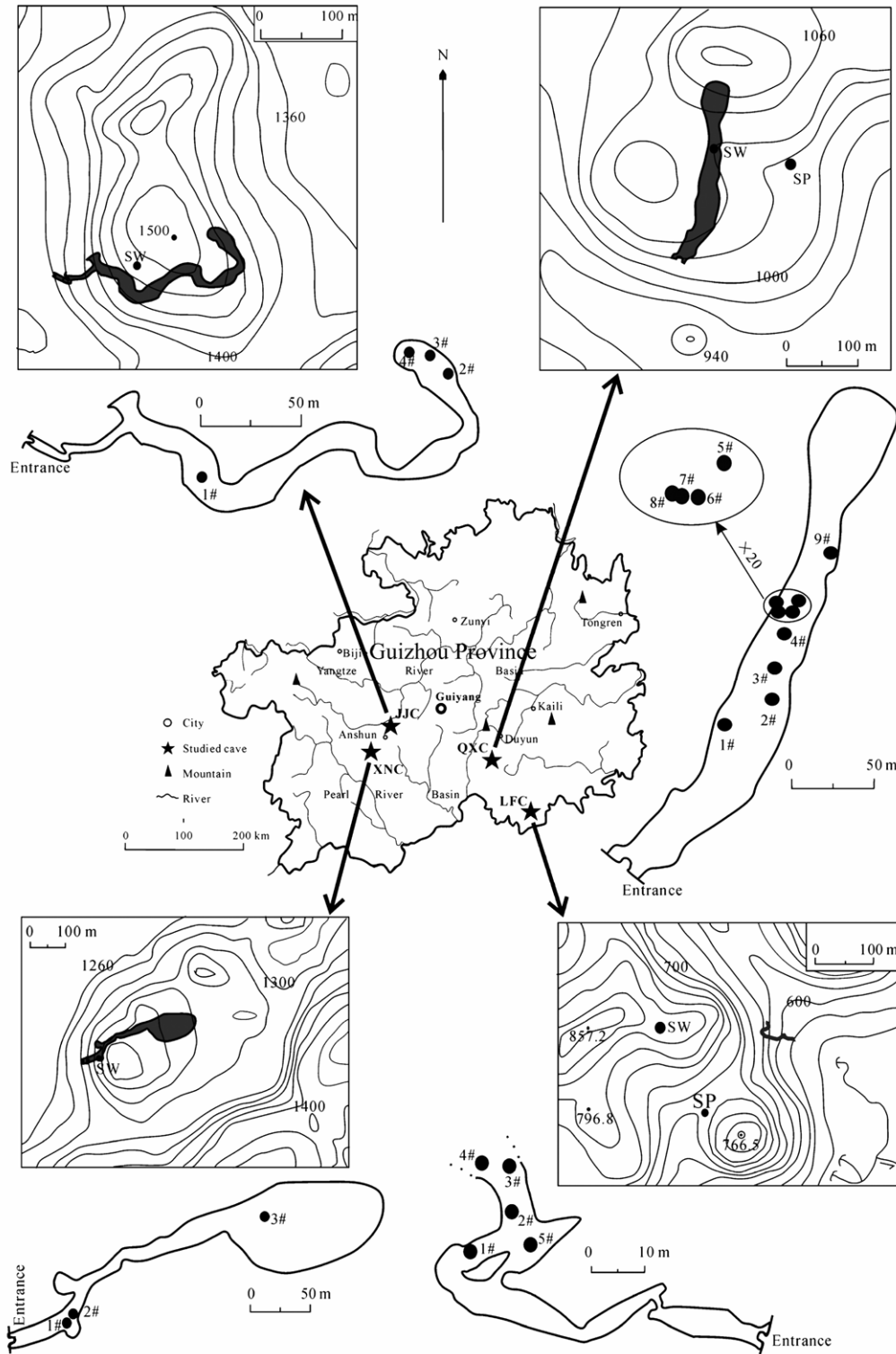


Fig. 1. Locations of the four caves. SW. Soil water; SP. spring water; 1#. drip water No. 1.

Drip rates were measured monthly at each drip site using a stop watch for 10 minutes at a time. Temperature, pH and HCO_3^- concentrations of water samples were measured *in-situ*. Their standard deviations were 0.1, 0.02°C, and <5%, respectively. Na^+ , K^+ , Ca^{2+} and Mg^{2+} concentrations were analyzed on an Atomic Absorption Spectrophotometer, and their

standard deviations were 0.1, 0.2, 5, and 2 mg/L, respectively. SO_4^{2-} and Cl^- concentrations were determined on a High Performance Liquid Chromatograph, with a precision of <5%. Sr^{2+} concentrations were analyzed by ICP-MS, with a precision of <5% as well. SI_C values were calculated by the WATSPAC Software using some of the parameters mentioned above. All

analytical processes were completed at the State Key Laboratory of Environmental Geochemistry, Institute of Geochemistry, Chinese Academy of Sciences.

4 Results and discussion

4.1 Drip rates

Fig. 3 and the results of our previous studies (Zhou Yunchao et al., 2005) show that among the five drip sites from LFC, drip rate was highest in 5#, followed by 3#, 1#, 4# and 2#, and their variation amplitudes were descending from 5#, 4#, 3#, 1# to 2#. In QXC, the average drip rates varied in the order of 4# > 5# > 8# > 6# > 1# > 2# > 3# > 7# > 9#, and the variation amplitudes followed the order of 4# > 9# > 6# > 7# > 2# > 3# > 8# > 5# > 1#. The drip rates displayed a large seasonal variation trend. That is, the drip rate was higher in rainy seasons than in dry seasons in 1# and 6#, especially in 6#. In JJC, the drip rate of 1# varied considerably with time, but was inconsistent with precipitation events; the drip rate of 2# was lower in rainy seasons than in dry seasons. As the three drip sites of XNC, the drip rate was lower in dry seasons than in rainy seasons. It varied in 1#, but was lowest in 2#. Therefore, based on the drip rates and their coefficients of variation, all 21 drip water sampling sites from the four caves can be divided into five groups (Fig. 3). The first group includes 1# and 3# of XNC whose drip rates and coefficients of variation are highest; the second group includes 5# of LFC, 4# of QXC and 1# of JJC; the third group includes 3# of LFC, 6#, 7#, 9# of QXC and 2# of JJC; the fourth group includes 1#, 4# of LFC, 2#, 3#, 5#, 8# of QXC; the fifth group includes 2# of LFC, 1# of QXC, 3# and 4# of JJC, and 2# of XNC.

4.2 Residence time

In this study, we used NaCl as a tracer to monitor the response of drip water to precipitation. There were 0.51 ± 0.22 ($n=6$) mg/L, 0.48 ± 0.27 ($n=10$) mg/L, 0.24 ± 0.11 ($n=3$) mg/L, 0.41 ± 0.06 ($n=3$) mg/L Cl^- in precipitation near the four caves between June and July 2003, which were lower than or close to the lowest values of their corresponding drip water samples. Our previous studies (Zhou Yunchao et al., 2005) showed that in LFC, Cl^- concentrations were highest in August 2003 in 1#, 4# and 5#, in September 2003 in 2#, and no peak appeared in 3#. Therefore, drip water in 2# responded most slowly to precipitation. Drip water in 6# of QXC responded quickly to precipitation. Drip water in 7# had the shortest response time to precipitation. In 4#, 6# and 9#, the largest Cl^- concentrations appeared in August 2003, and their response time to precipitation was relatively short.

Drip water in 1#, 2#, 5# and 8# had slower response (September 2003) to precipitation events, and that in 3# had the slowest response, where the largest Cl^- concentrations appeared in October 2003. In JJC, continuously monitored Cl^- concentrations showed that drip water responded quickly to precipitation in 1#, only 2 days (Zhou Yunchao et al., 2005), but the response time was about two months in 3# and 4#, and about three months in 2#. The Cl^- concentrations monitored continuously showed that the response time to precipitation events was 27 days in 1# of XNC (Zhou Yunchao et al., 2005), which was at least one month faster than that in the other two drip sites. Thus, it can be seen that those responding rates were coincident with the amplitudes of drip rate variation with time (Fig. 3). That is, the amplitudes of drip rate variation with time are large in those drip sites whose responding rates are relatively large.

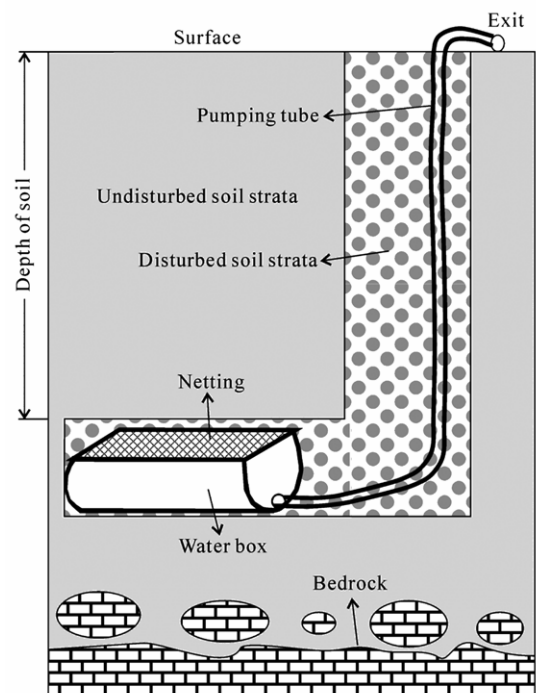


Fig. 2. Sketch of sampling soil water.

4.3 pH values

There was no significant difference in pH values of drip water in the same cave. However, there were significant differences not only among different types of water (such as soil water, spring water and drip water) in the same cave, but also in the same type of water from different cave systems (Table 2). The pH values of soil water increased slightly with soil depth, and they also increased with the downward movement of soil water, i.e., soil water < spring < drip water. The pH values of the three types of water from LFC were all lower than those of the other three caves (QXC,

JJC and XNC), whose pH values were similar, especially those of drip water. The pH values of precipitation were similar in the four cave areas with an average of >6. Our previous studies confirmed that the major organic substances (fulvic acid) in soil water and drip water had different characteristics under different vegetation coverages and biomass conditions (Xie Xingneng et al., 2008). For example, fulvic acid of drip water in LFC had longer excitation wavelength, which showed a higher humification degree of organic matter (Xie Xingneng et al., 2008). Therefore, this is one of the main factors that led to lower pH values of water in LFC than in the other cave systems. The pH values of drip water may also indicate changes in vegetation coverage/biomass under certain conditions.

4.4 Ion concentrations

In LFC, Na⁺, Ca²⁺, Mg²⁺, Sr²⁺, SO₄²⁻, Cl⁻, and HCO₃⁻ concentrations in soil water at the depth of 50 cm were lower than those at the depth of 100 cm (Table 2). Overall, there were no significant differences in concentrations and variations of ions for various drip sites in LFC (Table 2 and Fig. 4). The average Mg²⁺ and SO₄²⁻ concentrations were close to those of soil water at the depth of 50 cm in drip water and spring water except for 1# with very low SO₄²⁻, but the average Ca²⁺ concentrations were increasing from soil water at the depth of 50 to 100 cm, to drip water, and to spring water (Table 2). These results suggested that owing to pure limestone as bedrock in LFC, Mg came mainly from soil layer and Ca²⁺ from both soil layer and bedrock.

In XNC, Ca²⁺, Sr²⁺, HCO₃⁻ and SO₄²⁻ concentrations varied more greatly, and were larger in 1# and 2# than in 3# (Table 2 and Fig. 4). This might be affected by the response time of drip water to precipitation except for the strata with an interlayer of bedrock (T_{1a}: Lower Triassic Anshun Group) overlying XNC “dissolution collapse breccia of gypsum” (Bureau of Geology and Mineral Resources of Guizhou Province of China, 1987). Although the drip rate in 1# varied significantly with time, it did not synchronize with precipitation like the situation in 2# (Zhou Yunchao et al., 2005). However, the drip rate in 3# was not only large, but also corresponded well to precipitation. This implied that 1# and 2# may be mainly controlled by the piston flow, but 3# was controlled by preferential flow.

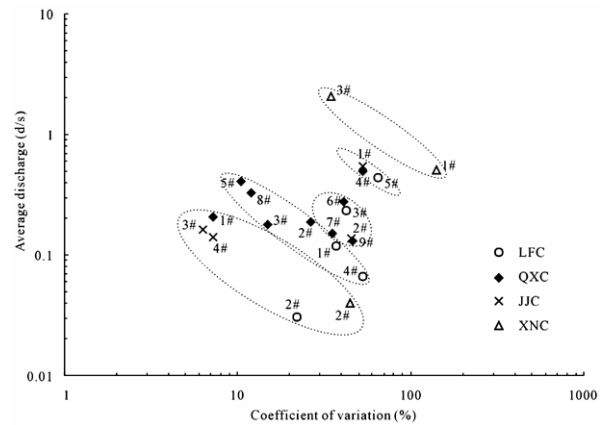


Fig. 3. Average discharge for the drip sites versus the coefficient of variation (standard deviation/mean×100). “Number #” indicates the number of drip site.

Table 2 The mean values of water temperature, hydrological parameter and the major ionic species of soil water, drip water and spring water

Sample No.	Group	T (°C)	Drip rate (d·s ⁻¹)	pH	K (mg·L ⁻¹)	Na (mg·L ⁻¹)	Ca (mg·L ⁻¹)	Mg (mg·L ⁻¹)	Cl (mg·L ⁻¹)	SO ₄ (mg·L ⁻¹)	HCO ₃ (mg·L ⁻¹)	SI _C ^b	Sr (μg·L ⁻¹)
LFS 50 ^c		22.1	- ^g	7.04	0.3	1.1	33.5	23.6	2.1	16.8	196.0	-0.6	15.8
mean		3.9	-	0.42	0.1	0.5	11.7	5.3	1.9	5.2	40.1	0.5	6.0
SD ^d		22.5	-	7.04	0.4	1.7	45.0	35.6	3.2	19.7	281.6	-0.4	20.9
LFS 100		4.0	-	0.35	0.3	1.2	21.7	7.2	1.3	4.4	72.6	0.6	4.1
mean		14.8	0.119	8.12	0.4	1.4	52.9	23.6	1.6	6.4	273.5	0.7	21.4
SD		1.3	0.044	0.36	0.1	1.0	11.4	1.8	0.2	0.5	36.0	0.4	2.8
LFC 2#		15.0	0.031	8.03	0.1	1.1	55.8	25.4	1.8	16.4	283.4	0.6	26.3
mean		1.4	0.007	0.48	0.0	0.5	12.8	1.6	0.4	0.8	34.2	0.5	6.0
SD		15.4	0.235	8.11	0.2	0.9	50.6	22.5	1.1	11.1	262.0	0.6	20.9
LFC 3#		0.8	0.100	0.40	0.1	0.4	10.7	1.2	0.3	2.2	27.0	0.4	4.6
mean		15.0	0.066	8.03	0.1	1.0	53.3	24.9	1.5	14.5	275.4	0.5	27.8
SD		1.4	0.035	0.41	0.1	0.4	30.2	1.7	0.3	1.2	76.2	0.5	10.2
LFC 4#		14.9	0.440	8.10	0.2	0.9	51.8	24.1	1.5	12.5	274.2	0.6	21.1
mean		1.3	0.286	0.34	0.0	0.4	5.6	0.9	0.5	1.0	27.4	0.4	3.1
SD													

(to be continued)

Table 2 (continued)

Sample No.	Group	T (°C)	Drip rate (d·s ⁻¹)	pH	K (mg·L ⁻¹)	Na (mg·L ⁻¹)	Ca (mg·L ⁻¹)	Mg (mg·L ⁻¹)	Cl (mg·L ⁻¹)	SO ₄ (mg·L ⁻¹)	HCO ₃ (mg·L ⁻¹)	SI _c ^b	Sr (μg·L ⁻¹)
LFC SP ^f		17.7	-	7.60	0.1	1.0	64.4	24.0	1.0	11.2	305.2	0.3	26.3
mean		2.0	-	0.32	0.0	0.6	18.3	8.0	0.3	2.1	65.5	0.4	7.7
SD		23.0	-	7.55	0.3	1.5	28.7	14.5	2.6	13.3	149.4	-0.3	16.9
QXS 50		4.8	-	0.27	0.1	1.4	4.3	3.3	1.9	8.7	24.4	0.2	4.2
mean		22.3	-	7.64	0.4	1.9	45.2	17.7	2.1	18.3	213.8	0.0	21.7
SD		5.7	-	0.60	0.4	0.9	18.5	3.6	0.9	7.7	63.9	0.4	6.5
QXC 1#		13.6	0.208	8.32	0.2	0.9	23.8	26.5	0.4	9.3	200.3	0.3	16.9
mean		1.3	0.015	0.42	0.1	0.6	15.2	1.5	0.3	0.7	41.9	0.5	2.4
SD		13.7	0.187	8.41	0.2	0.8	25.6	28.8	0.8	6.8	223.3	0.5	17.1
QXC 2#		1.5	0.049	0.43	0.1	0.5	7.9	2.3	0.5	0.3	22.7	0.5	4.9
mean	I	13.4	0.276	8.45	0.3	0.8	19.6	29.0	0.8	8.0	200.4	0.4	8.2
SD		1.3	0.113	0.28	0.1	0.4	8.8	1.0	0.4	0.4	21.9	0.4	3.1
QXC 6#		13.1	0.151	8.33	0.3	0.7	31.7	29.4	0.7	8.1	236.0	0.5	13.8
mean		1.5	0.053	0.34	0.2	0.5	21.5	3.5	0.4	0.5	60.3	0.5	4.8
SD		13.4	0.328	8.40	0.2	0.7	28.6	28.6	1.2	7.8	223.3	0.5	15.2
QXC 7#		1.4	0.039	0.33	0.1	0.4	10.6	0.8	1.5	0.6	26.4	0.4	4.0
mean		13.8	0.179	8.36	0.3	0.9	33.7	28.3	0.8	5.0	249.3	0.6	22.7
SD		1.4	0.027	0.33	0.1	0.6	9.5	1.1	0.5	0.4	29.9	0.4	3.7
QXC 3#		13.7	0.498	8.38	0.3	0.8	41.1	28.0	0.7	6.0	265.7	0.7	21.0
mean	II	1.3	0.264	0.31	0.1	0.5	16.0	2.5	0.2	1.1	40.1	0.4	7.3
SD		13.5	0.404	8.29	0.2	0.7	50.5	29.7	0.8	7.6	298.0	0.8	20.9
QXC 4#		1.5	0.042	0.29	0.1	0.4	21.8	3.1	0.4	0.7	54.7	0.5	7.2
mean		13.8	0.130	8.36	0.2	0.6	43.6	24.9	0.8	11.8	248.8	0.7	36.7
SD		1.3	0.060	0.27	0.1	0.4	19.0	1.5	0.4	0.7	45.2	0.3	8.1
QXC 5#		17.3	-	8.06	0.2	0.8	41.6	23.7	1.2	16.4	234.7	0.4	25.5
mean		2.4	0.37	0.2	0.4	13.6	4.1	0.5	6.6	49.7	0.5	2.7	
SD		22.2	-	7.36	0.6	9.2	39.5	17.8	20.9	37.0	148.9	-0.4	34.2
JJS 50		2.7	0.24	0.3	6.3	9.9	3.5	16.3	4.9	41.0	0.4	14.8	
mean		28.3	-	8.04	3.4	4.6	54.3	18.5	8.6	32.1	198.1	0.7	-
SD		0.0	-	0.00	0.0	0.0	0.0	0.0	0.0	0.0	0.0	0.0	-
JJS 100		15.7	0.546	8.32	0.4	1.5	39.1	21.5	4.0	29.7	190.4	0.6	22.6
mean	II	3.5	0.288	0.47	0.6	1.1	2.8	1.8	2.8	5.5	13.5	0.5	5.8
SD		16.4	0.141	8.33	0.1	0.5	40.1	19.4	0.6	4.0	222.1	0.7	35.1
JJC 1#		3.2	0.010	0.52	0.0	0.2	9.1	1.1	0.3	0.3	20.7	0.6	9.5
mean		16.4	0.136	8.35	0.2	0.6	18.7	20.3	0.9	4.9	156.0	0.2	9.1
SD		3.2	0.061	0.53	0.1	0.3	2.0	1.4	1.0	0.5	11.3	0.5	1.9
JJC 2#		16.4	0.164	8.40	0.2	0.5	21.1	20.0	0.6	4.4	165.4	0.4	10.2
mean	I	3.3	0.010	0.58	0.3	0.3	3.5	1.3	0.2	0.4	18.8	0.5	3.1
SD		24.2	-	7.09	0.2	1.0	36.4	21.3	2.3	12.9	188.9	-0.6	20.5
XNS 50		2.8	-	0.10	0.1	0.2	14.6	8.0	0.4	3.7	83.2	0.3	10.4
mean		17.3	0.503	8.29	0.3	0.6	67.8	50.2	1.2	33.5	422.7	1.0	21.3
SD		2.4	0.704	0.40	0.3	0.2	29.2	2.7	1.1	1.9	88.5	0.7	11.4
XNC 1#		18.0	0.040	8.40	0.3	0.6	50.2	54.6	2.1	30.5	415.0	1.0	28.3
mean		2.9	0.018	0.26	0.2	0.2	27.1	5.5	3.8	1.1	93.9	0.4	13.7
SD		18.1	2.083	8.38	0.2	0.4	44.7	27.2	0.7	18.2	263.5	0.8	17.9
XNC 2#		1.7	0.724	0.42	0.2	0.1	8.5	1.0	0.5	0.4	32.2	0.4	4.3
mean													
SD													

Note: ^b Saturation index for calcite; ^c soil water at the 50 cm soil depth; ^d standard deviation; ^e No.1 drip site, the rest can be deduced by analogy; ^f spring water;

^g No data.

In QXC and JJC, Na^+ , Ca^{2+} , Mg^{2+} , Sr^{2+} , SO_4^{2-} , Cl^- and HCO_3^- concentrations in soil water were also lower at the depth of 50 cm than at the depth of 100 cm (Table 2 and Fig. 4). Ca^{2+} , Sr^{2+} and HCO_3^- concentrations were significantly lower in Group I than in Group II, and Ca^{2+} , Sr^{2+} concentrations in Group I were not higher than those of soil water at the depth of 50 cm and those in Group II between 50 cm and 100 cm. Mg^{2+} concentrations were slightly higher in 9# than those of soil water at the depth of 100 cm, but lower than those at the other eight drip sites in QXC, among which there were no significant differences. Sr^{2+} and Ca^{2+} concentrations were lowest in 6# of QXC, and highest in 9#. Sr^{2+} concentrations were significantly higher in 4# of JJC than those in the other three drip water sites. SO_4 concentrations were not the same for different drip water sites in QXC and JJC. In QXC, ion concentrations in 9# were highest (similar to those of soil water at the depth of 100 cm), followed by 1#, those in 2# and 4# were similar to each other and low, those in 3# were lowest, and those in the other four sites were close to each other and at the intermediate level. In JJC, ion concentrations in 1# were larger than those in the other three sites which were close to each other. In the spring water near QXC, Na^+ , K^+ , Ca^{2+} , Mg^{2+} , Sr^{2+} , SO_4^{2-} , Cl^- , HCO_3^- concentrations were between those of soil water at the depth of 100 cm and those of drip water in 9# (Table 2 and Fig. 4). These indicated that the substances in drip water were derived mainly from the soil layer; Group I in QXC and JJC might pass through a thinner soil layer (less than 50 cm) than Group II (more than 50 cm), especially 9# of QXC, which was thickest; 6# might be affected by preferential flow. So far, variations in SO_4^{2-} concentrations in drip water are hard to understand, so further study needs to be done.

4.5 Prior calcite precipitation

Prior calcite precipitation (PCP) in the percolation routes overlying the cave is the most probable process that controls Ca^{2+} variation in drip water. Ca^{2+} depletion by prior calcite precipitation occurs preferentially under certain conditions (Karmann et al., 2007) where the partition coefficient of Mg [$K_{\text{Mg}} = (\text{Mg}/\text{Ca})_{\text{calcite}}/(\text{Mg}/\text{Ca})_{\text{solution}}$] is much lower than unity. This condition results in a larger reduction in Ca than in Mg. Hence, the Mg/Ca ratio increases in solution (Fairchild and Treble, 2009; Gascoyne, 1983; Huang and Fairchild, 2001) and in drip water. Therefore, under certain geological conditions, a large Mg/Ca ratio indicates a large degree of PCP (Fairchild et al., 2000; Fairchild et al., 2006). Fig. 5 shows that the Mg/Ca ratios are higher in Group I than in Group II in QXC and JJC and not lower than those of soil

water. However, in LFC and XNC, the Mg/Ca ratios of drip water are similar to those of soil water. These results suggested that PCP did not happen or only slightly happened in LFC and XNC, but the degree of PCP was relatively high in QXC and JJC, especially in Group I.

4.6 Calcite saturation indices

There was no significant temporal variation in SI_C for the four caves, but spatial variations were distinct. The SI_C value of drip water of XNC was highest and that of Group I of QXC and JJC was lowest. The SI_C value of soil water was lower at the depth of 50 cm than at the depth of 100 cm, and its values indicated that soil water was unsaturated in the LFC system (Table 2). The SI_C values of drip water were also close to each other in LFC. The SI_C value of spring water varied nearly between that of soil water and that of drip water (Table 2), which was similar to pH value. The average SI_C value of soil water at the depth of 50 cm also indicated unsaturation in XNC. SI_C was larger in 1# and 2# than in 3# (Table 2), the same as Ca and HCO_3^- . The SI_C value of soil water at the depth of 50 cm was also lower than that at the depth of 100 cm, and its values indicated that some soil water was saturated in QXD and JJC. In the spring near QXC, SI_C values were close to those of Group I, and between those of soil water at the depth of 100 cm and those of drip water in 9# (Table 2). These characteristics of SI_C showed that the dissolution ability of percolation water to calcite decreased significantly from soil water to drip water; conversely, the SI_C values of Group I were lower, and those of some drip water samples were even lower than zero. Therefore, these speleothems formed from drip water with lower SI_C values may not be ideal geological archives because of a slow calcite precipitation rate and only partial dissolution.

In conclusion, based on our research on the hydro-geochemistry parameters for drip water, in combination with the results of previous studies (Tooth and Fairchild, 2003), the 21 drip water sites are classified as five categories, I, II, III, IV, and V (Table 3), which are consistent with what is described in Section 4.1 (Fig. 3).

4.7 Implications

Results of this study showed that there were greatly different hydro-geochemical characteristics for adjacent drip water sites in the same cave as QXC and JJC, but not in LFC and XNC. The above analysis showed that these different hydro-geochemical characteristics resulted from different geochemical processes,

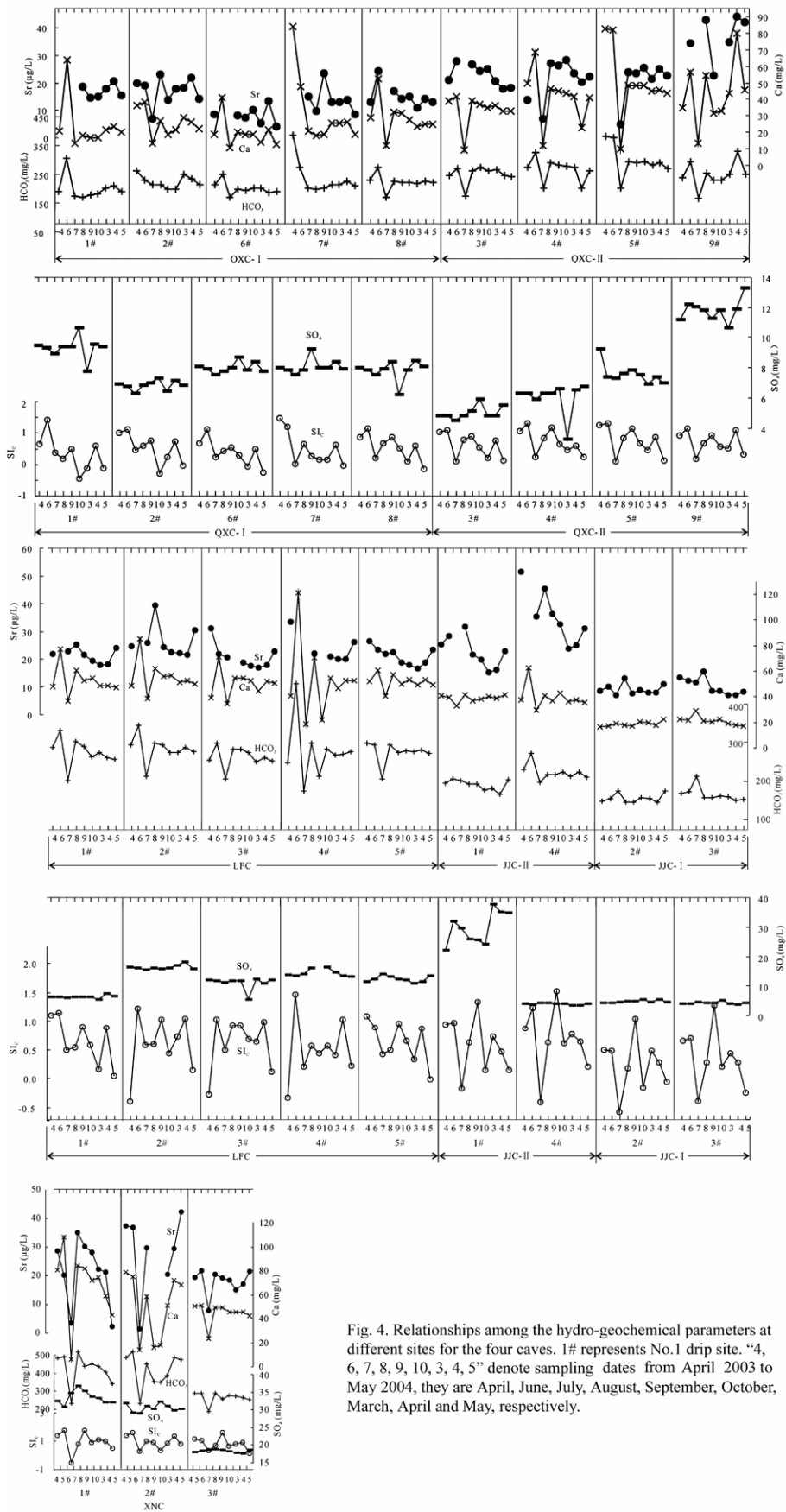


Fig. 4. Relationships among the hydro-geochemical parameters at different sites for the four caves. 1# represents No.1 drip site. "4, 6, 7, 8, 9, 10, 3, 4, 5" denote sampling dates from April 2003 to May 2004, they are April, June, July, August, September, October, March, April and May, respectively.

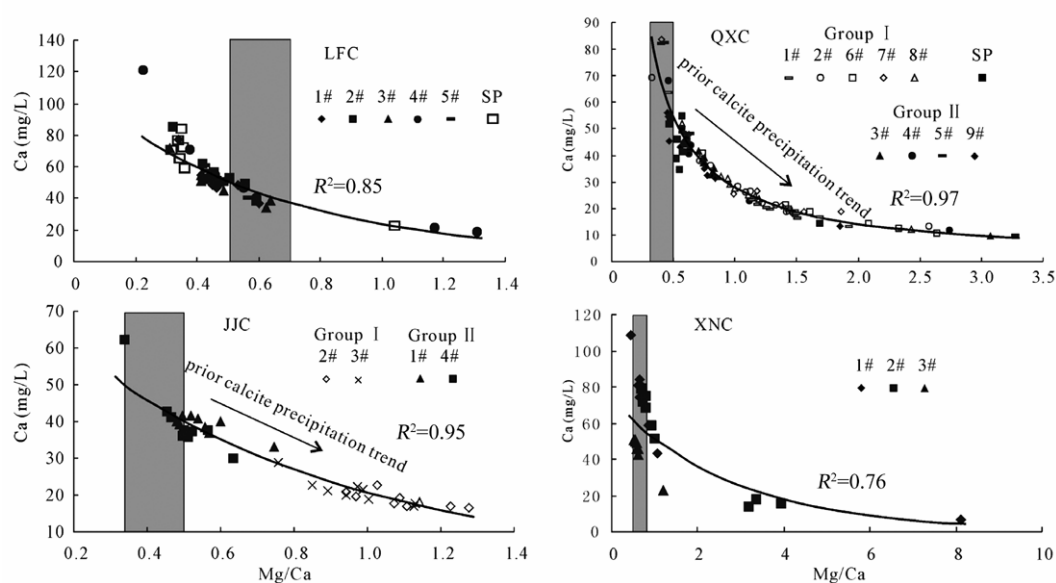


Fig. 5. Correlations between Ca and Mg/Ca (the grey column represents the Mg/Ca range of soil water).

Table 3 Summary of hydro-geochemical responses to recharge of karst water in the four caves and the details of associated speleothem forms at each site

Cave	Site	Drip rate change	Response time/month (\leq) (Cl)	Prior calcite precipitation	Speleothem	Water head change	Flow type*
LFC	1#	Large	2	No	Yes	No	IV
	2#	Slight	3	No	Yes	No	V
	3#	Large	2–3	No	Yes	Slight	III*
	4#	Large	2	No	Yes	No	IV
	5#	Large	2	No	Yes	Yes	II
QXC	1#	Few	3	Yes	Yes	No	V
	2#	Slight	2–3	Yes	Less	Few	IV
	3#	Slight	4	Slight	Yes	Few	IV
	4#	Large	2	Slight	Yes	Yes	II
	5#	Slight	3	Slight	Yes	Few	IV
	6#	Large	2	Yes	Yes	Slight	III
	7#	Large	1	Yes	Yes	Slight	III
	8#	Slight	3	Yes	Yes	Few	IV
	9#	Large	2	Slight	Yes	Slight	III
JJC	1#	Large	1	Slight	Less	Yes	II
	2#	Large	3	Yes	Seldom	Slight	III*
	3#	Few	2	Yes	Seldom	No	V
	4#	Few	2	Slight	Yes	No	V
XNC	1#	Very large	1	No	Yes	Yes	I*
	2#	Slight	3	No	Yes	No	V*
	3#	Large	2	No	Yes	Yes	I

* They are probably controlled by piston flow. I. Preferential flow; II. preferential flow with matrix flow; III. preferential flow and matrix flow; IV. matrix flow with preferential flow; V. matrix flow.

which included mainly bedrock dissolution and PCP processes and were restricted by hydrological processes. Hydrological processes were controlled by the physical and chemical properties of the epikarst. Therefore, hydrological conditions played an important role in the evolution of various geochemical indicators in the cave systems and further controlled the geochemical characteristics of the corresponding speleothem, including stable carbon isotopic composition. It was suggested that carbon isotopic composition was not only affected by vegetation types (C3/C4 ratio) and vegetation coverage (biomass) as commonly accepted, but also by other hydro-geochemical characteristics. In other words, the simple conventional model of environment changes reconstructed only by Mg/Ca ratios and the variations in $\delta^{13}\text{C}$ was debatable. This study and its companion (unpublished data) revealed that, as for the same environment, there were significant correlations between the $\delta^{13}\text{C}_{\text{DIC}}$ values of drip water (i.e., speleothem) and other hydro-geochemical parameters, especially drip rate, Ca^{2+} , Sr^{2+} , HCO_3^- , Mg/Ca ratio and SI_C . Therefore, if the impacts of hydro-geochemical processes on $\delta^{13}\text{C}$ were ignored, then the interpretation of ecological environment only using the $\delta^{13}\text{C}$ values of speleothem would be inaccurate.

5 Conclusions

This study shows that there are significant hydro-geochemical differences for the 21 drip water sampling sites from the four caves of Guizhou, Southwest China, due to heterogeneous media overlying the same cave, which may lead to different flow paths of seepage water in the epikarst. The 21 sites are classified as five categories based on hydro-geochemical variations in drip water. These hydro-geochemical differences may be the result of different residence time and microenvironments of seepage water in the migration path inside the soil layer and the bedrocks overlying different caves. However, the hydro-geochemistry plays an important role in the evolution of various geochemical indicators in the cave systems, and further controls the geochemical characteristics of the corresponding speleothem. Therefore, the hydro-geochemical effects on some proxy indices cannot be ignored when a paleo-environment is reconstructed using speleothem calcite.

Acknowledgements The research project was funded jointly by the Orientation Project of Knowledge Innovation Program sponsored by the Chinese Academy of Sciences (No. kzcx2-yw-306) and the National Natural Science Foundation of China (Nos.

41003054 and 90202003). The authors wish to thank Profs. Ran Jingcheng (Maolan National Nature Reserve Administration) and Rong Li (Guizhou Normal University) for their assistance in the field work. Sincere thanks are also due to Prof. Tan Ming and editors for their valuable comments and suggestions for improving the manuscript.

References

- Baker A. and Bradley C. (2010) Modern stalagmite $\delta^{18}\text{O}$: Instrumental calibration and forward modelling [J]. *Global and Planetary Change*. **71**, 201–206.
- Baldini J.U.L., McDermott F., and Fairchild I.J. (2006) Spatial variability in cave drip water hydrochemistry: Implications for stalagmite paleoclimate records [J]. *Chemical Geology*. **235**, 390–404.
- Bradley C., Baker A., Jex C.N. et al. (2010) Hydrological uncertainties in the modelling of cave drip-water $\delta^{18}\text{O}$ and the implications for stalagmite palaeoclimate reconstructions [J]. *Quaternary Science Reviews*. **29**, 2201–2214.
- Bureau of Geology and Mineral Resources of Guizhou Province of China (1987) *Regional Geology of Guizhou Province* [R]. Geological Publishing House, Beijing (in Chinese).
- Dreybrodt W. (1988) *Processes in Karst Systems, Physics, Chemistry, and Geology* [M]. New York, NY (USA), Springer-Verlag.
- Dykoski C.A., Edwards R.L., Cheng H. et al. (2005) A high-resolution, absolute-dated Holocene and deglacial Asian monsoon record from Dongge Cave, China [J]. *Earth and Planetary Science Letters*. **233**, 71–86.
- Fairchild I.J., Borsato A., Tooth A.F. et al. (2000) Controls on trace element (Sr-Mg) compositions of carbonate cave waters: Implications for speleothem climatic records [J]. *Chemical Geology*. **166**, 255–269.
- Fairchild I.J. and Treble P.C. (2009) Trace elements in speleothems as recorders of environmental change [J]. *Quaternary Science Reviews*. **28**, 449–468.
- Fairchild I.J., Tuckwell G.W., Baker A. et al. (2006) Modelling of dripwater hydrology and hydrogeochemistry in a weakly karstified aquifer (Bath, UK): Implications for climate change studies [J]. *Journal of Hydrology*. **321**, 213–231.
- Ford D.C. and Williams, P. (2007) *Karst Hydrogeology and Geomorphology* [M]. New York, John Wiley and Sons.
- Gascoyne M. (1983) Trace-element partition coefficients in the calcite-water system and their paleoclimatic significance in cave studies [J]. *Journal of Hydrology*. **61**, 213–222.
- He Yaoqi, Wang Yongjin, Kong Xinggong et al. (2005) High resolution stalagmite $\delta^{18}\text{O}$ records over the past 1000 years from Dongge Cave in Guizhou [J]. *Chinese Science Bulletin*. **50**, 1003–1008.
- Huang Y. and Fairchild I.J. (2001) Partitioning of Sr^{2+} and Mg^{2+} into calcite under karst-analogue experimental conditions [J]. *Geochimica et Cosmochimica Acta*. **65**, 47–62.
- Karmann I., Cruz Jr F.W., Viana Jr O. et al. (2007) Climate influence on geochemistry parameters of waters from Santana-Perolas cave system, Brazil [J]. *Chemical Geology*. **244**, 232–247.
- Kelly M.J., Edwards R.L., Cheng H. et al. (2006) High resolution characterization of the Asian Monsoon between 146000 and 99000

- years B.P. from Dongge Cave, China and global correlation of events surrounding Termination II [J]. *Palaeogeography, Palaeoclimatology, Palaeoecology*. **236**, 20–38.
- Lambert W.J. and Aharon P. (2010) Oxygen and hydrogen isotopes of rainfall and dripwater at DeSoto Caverns (Alabama, USA): Key to understanding past variability of moisture transport from the Gulf of Mexico [J]. *Geochimica et Cosmochimica Acta*. **74**, 846–861.
- Lambert W.J. and Aharon P. (2011) Controls on dissolved inorganic carbon and $\delta^{13}\text{C}$ in cave waters from DeSoto Caverns: Implications for speleothem $\delta^{13}\text{C}$ assessments [J]. *Geochimica et Cosmochimica Acta*. **75**, 753–768.
- Linge H., Lauritzen S.E., Lundberg J. et al. (2001) Stable isotope stratigraphy of Holocene speleothems: Examples from a cave system in Rana, northern Norway [J]. *Palaeogeography, Palaeoclimatology, Palaeoecology*. **167**, 209–224.
- McDonald J. and Drysdale R. (2007) Hydrology of cave drip waters at varying bedrock depths from a karst system in southeastern Australia [J]. *Hydrological Processes*. **21**, 1737–1748.
- McDonald J., Drysdale R., Hill D. et al. (2007) The hydrochemical response of cave drip waters to sub-annual and inter-annual climate variability, Wombeyan Caves, SE Australia [J]. *Chemical Geology*. **244**, 605–623.
- Serefiddin F., Schwarcz H.P., Ford D.C. et al. (2004) Late Pleistocene paleoclimate in the Black Hills of South Dakota from isotope records in speleothems [J]. *Palaeogeography, Palaeoclimatology, Palaeoecology*. **203**, 1–17.
- Spötl C., Fairchild I.J., and Tooth A.F. (2005) Cave air control on dripwater geochemistry, Obir Caves (Austria): Implications for speleothem deposition in dynamically ventilated caves [J]. *Geochimica et Cosmochimica Acta*. **69**, 2451–2468.
- Tooth A.F. and Fairchild I.J. (2003) Soil and karst aquifer hydrological controls on the geochemical evolution of speleothem-forming drip waters, Crag Cave, Southwest Ireland [J]. *Journal of Hydrology*. **273**, 51–68.
- Wang Y., Cheng H., Edwards R.L. et al. (2005) The Holocene Asian Monsoon: Links to solar changes and North Atlantic climate [J]. *Science*. **308**, 854–857.
- Wang Zhaorong, Peng Zicheng, Ni Shoubin et al. (1999) Progress in speleothem stalagmite paleoclimatology and chronology [J]. *Chinese Journal of Geochemistry*. **18**, 25–29.
- Wang Zhaorong, Yuan Daoxian, Lin Yushi et al. (2001) High-resolution dating of stalagmites and reconstruction of paleo-environments [J]. *Chinese Journal of Geochemistry*. **20**, 282–288.
- Xie Xingneng, Wang Shijie, Zhou Yunchao et al. (2008) Three-dimensional fluorescence spectral characteristics of dissolved organic carbon in cave drip waters and their responses to environment changes: Four cave systems as an example in Guizhou Province, China [J]. *Chinese Science Bulletin*. **53**, 884–889.
- Yuan D., Cheng H., Edwards R.L. et al. (2004) Timing, Duration, and Transitions of the Last Interglacial Asian Monsoon [J]. *Science*. **304**, 575–578.
- Zhou Yunchao, Wang Shijie, Xie Xingneng et al. (2005) Significance and dynamics of drip water responding to rainfall in four caves of Guizhou, China [J]. *Chinese Science Bulletin*. **50**, 154–161.